EANDC (OR) - 93 "L"

INDC (SWT) - 1 "G"

PROGRESS REPORT TO EANDC FROM SWITZERLAND

June 1970

Edited by

T. Hürlimann

Swiss Federal Institute for Reactor Research

Würenlingen

~~NOT FOR PUBLICATION~~

INTRODUCTION

This progress report contains information of work done in the neutron cross section field at various Swiss laboratories during the last year. The information is not intended ot be complete, nor does it cover all of the work in the reporting laboratories relating to nuclear cross section measurements. As some of the data, which appear in this report are of preliminary character, they must not be quoted in publications without permission of the experimenter associated with the work.

CONTENTS

		page
I.	Institut de Physique, Université de Neuchâtel	1
II.	Physikalisches Institut der Universität Basel	16
III.	Institut de Physique Nucléaire, Université de Lausanne	24
IV.	Eidgenössisches Institut für Reaktorforschung, Würenlingen	26

I. Institut de Physique, Université de Neuchâtel

(Dir.: Prof. Dr. Jean Rossel)

1. Excitation Function for (n, p) and (n,α) Reactions with ^{28}Si and ^{29}Si

F. Foroughi and J. Durisch

For the simultaneous study of the angular distribution of the product nuclei in ^{29}Si(n, α)^{26}Mg and ^{29}Si(n, p)^{29}Al we need the corresponding excitation functions for which the published data present contradiction [1-3]. To get reliable results we used a Si surface barrier counter both as target and detector, with careful monitoring of the active depth (450 μm with 3 cm^2 surface and an α-resolution of 25 keV). Peaks for ^{29}Si(n, α_k) with k = 0, 1 and 2; ^{28}Si(n, α_o)^{25}Mg and ^{28}Si(n, p_o+p_1)^{28}Al have been observed for neutron energies between 5.2 and 6.2 MeV (Fig. 1). The energy reso-

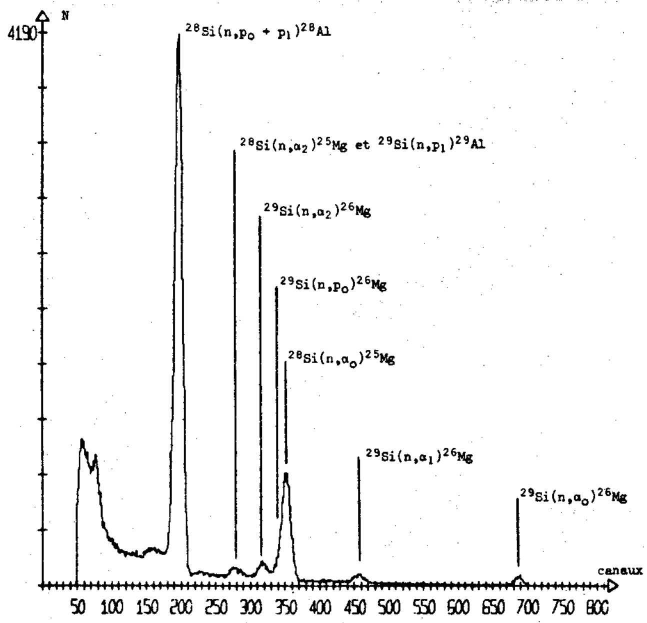

Fig. 1:

Particle spectrum of the (n,α)- and (n, p) reactions on ^{28}Si and ^{29}Si.

lution of the incident neutron of 38 keV is due to deuton straggling in the window and in the deuterium gas of the targets (p = 100 mm Hg) and also to the angular spread of the neutron beam ($< 2^{o}$).

The reverse current of the detector diode determines the bias V. Its fluctuations affect the effective depth ($\sim \sqrt{V}$) of the sensitive Si material target layer. During all the measurements this current was stable within 5%. The exact relation between counting rate and bias voltage V has been investigated in [4], so it was possible to normalize the experimental values to the effective depth.

The cross sections given in the figures are only tentative (no edge effect could be taken into account due to the unknown angular distributions).

Figures 2 to 8 give the measured cross sections. Below 5.8 MeV the

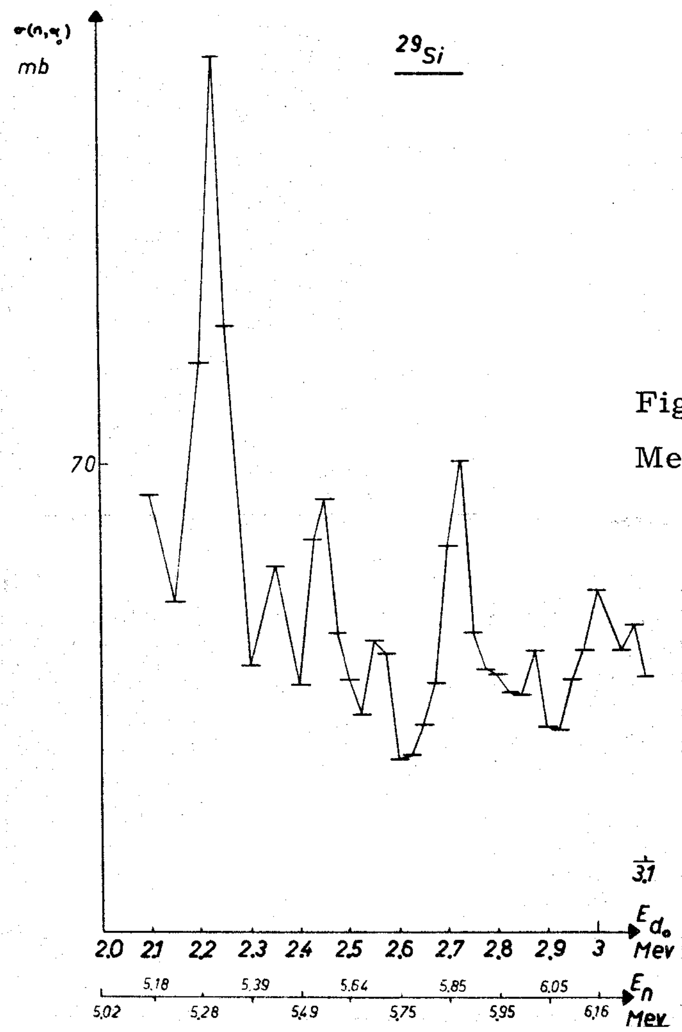

Fig. 2:
Measured $^{29}Si(n,\alpha_{o})$ cross section.

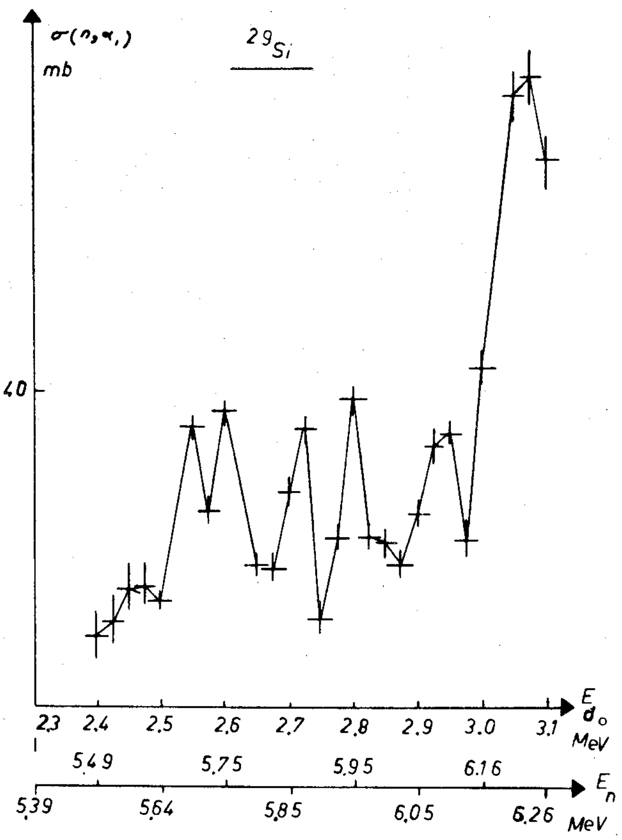

Fig. 3:

Measured $^{29}Si(n,\alpha_1)$ cross section.

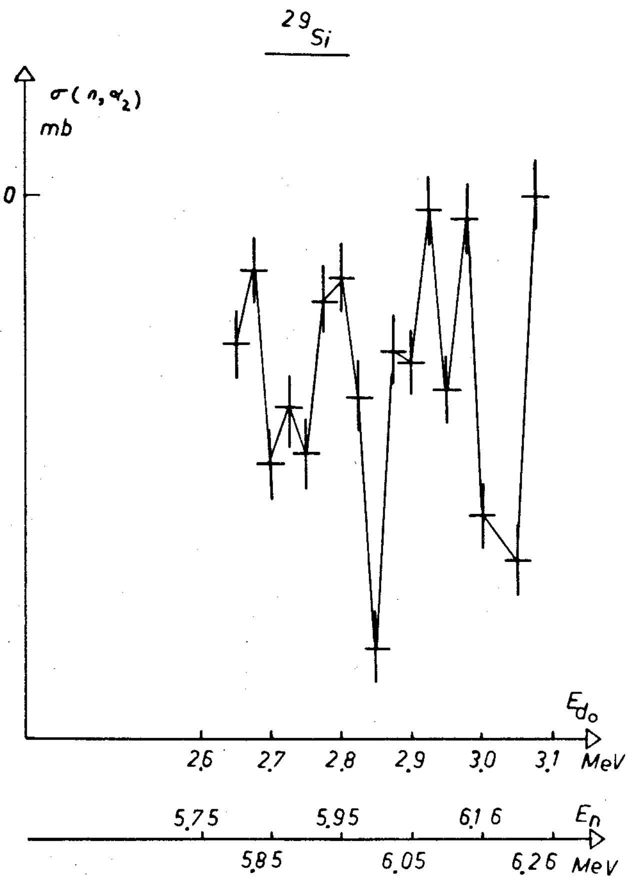

Fig. 4:

Measured $^{29}Si(n,\alpha_2)$ cross section.

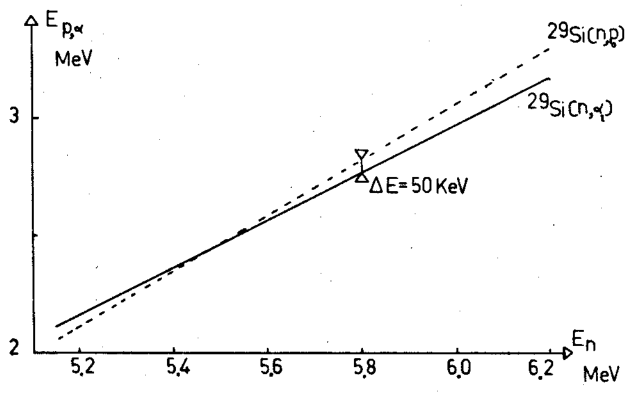

Fig. 5:

Variation of proton and alpha particle energy with incident neutron energy.

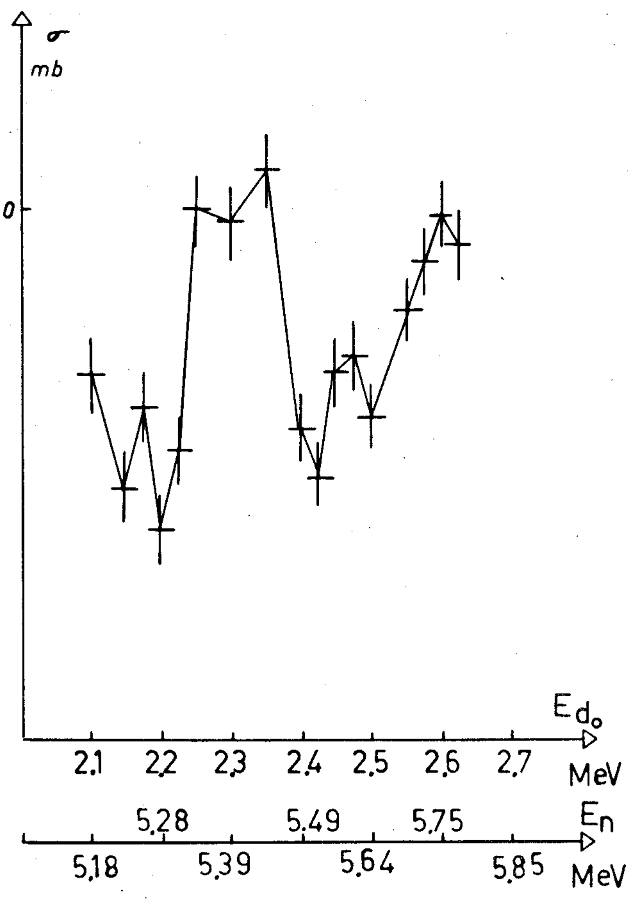

Fig. 6:

Measured combined cross section for the $^{29}Si(n,\alpha_2)$ and $^{29}Si(n,p_0)$ reaction.

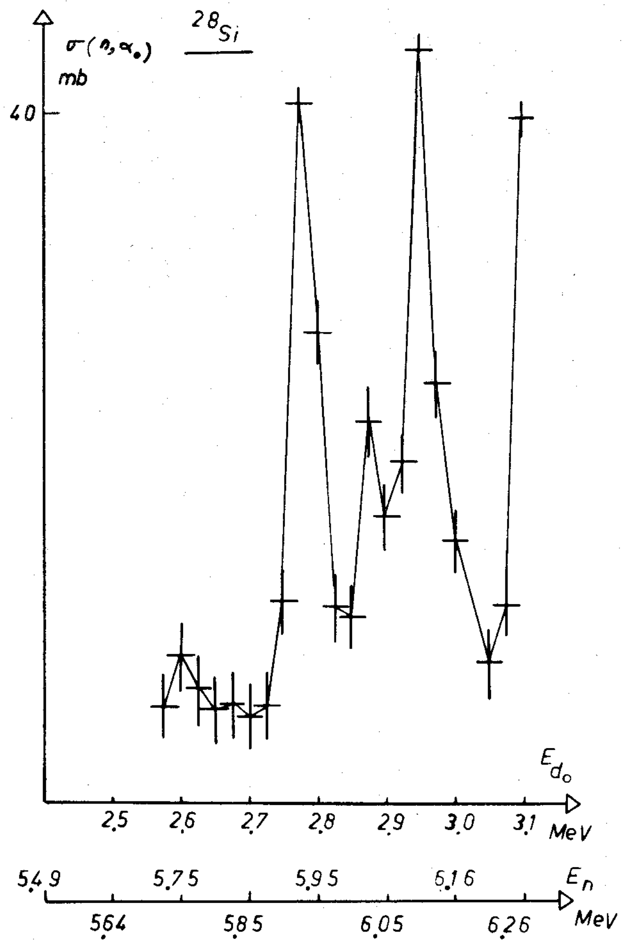

Fig. 7:
Measured $^{28}Si(n,\alpha_0)$ cross section.

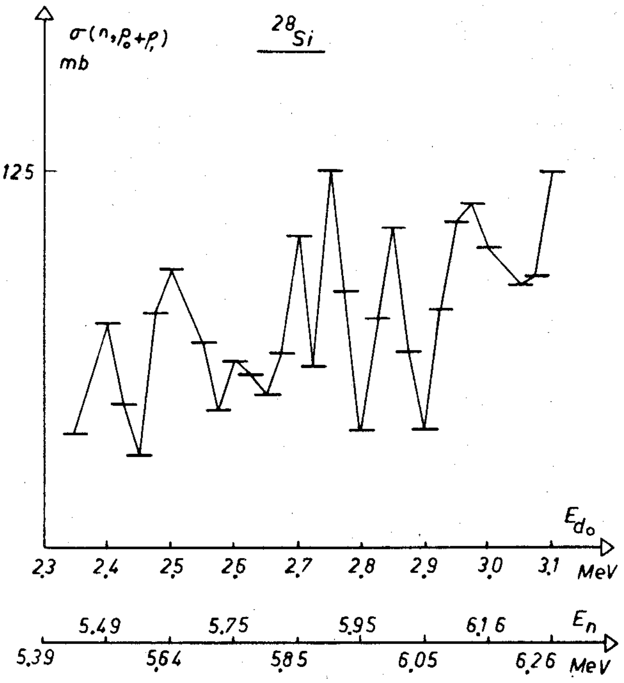

Fig. 8:
Measured $^{28}Si(n,p_0+p_1)$ cross section.

proton peak of ^{29}Si cannot be distinguished from the α_2 peak of ^{29}Si (Fig. 5). Therefore Fig. 6 shows the continuation of the measurement without identification.

The excitation function for $^{29}Si(n,\alpha_0)^{26}Mg$ only is in agreement with that given in [1] , but different of that presented in [2] and [3] . Our other results differ from those of [1-3] . The α_2 of the ^{29}Si reaction have already been identified [1-3] but the corresponding excitation function was not given.

From the table [5] the level density may be estimated in the Fermi gas model, giving approximately 1 level/keV in ^{30}Si and approx. 1 level/3 keV in ^{28}Si: in the energy region of excitation. Considering these values and the probable level width, it seems probable that part of the observed maxima (especially in ^{30}Si) correspond to the Ericson fluctuations.

This work has been supported by the "Fonds National Suisse de la Recherche Scientifique".

References

[1] G. Anderson-Lindström, G. Betz, W. Mansberg, E. Rössle Mém. Soc. Roy. Sci. Liège 30, 265 (1964)

[2] R. Potenza, R. Ricamo, A. Rubbino, N.P. 41, 298 (1963)

[3] B. Mainsbridge, T.W. Bonner, T.A. Rabson, N.P. 48, 83 (1963)

[4] J.E. Durisch, F. Foroughi, J. Rossel, N. Inst. Meth. 52, 222 (1967)

[5] A. Gilbert, G.W. Cameron, Can. Journ. Phys. 43, 1446 (1965)

2. A Complete Experiment on the Reaction D(n, nnp) at 14 MeV

C. Lunke, J.-P. Egger and J. Rossel

This is the final report on an experiment described in the progress report of last year [EANDC(OR)-90, pg. 16] .

For the chosen configuration (Fig. 9) the relative energy E_{13} between neutron (30^{o}) and proton is small. This is favorable to extract a reliable value for the scattering length a^{s}_{np} for the n-p final state interaction of the 3 body process.

A fourfold coïncidence (α, p, n_1, n_2) ensures a good selection of the useful events ($\sim 1/10^{9}$) and a 3-parametric measurement of $\vec{p}_1$, $\vec{p}_2$

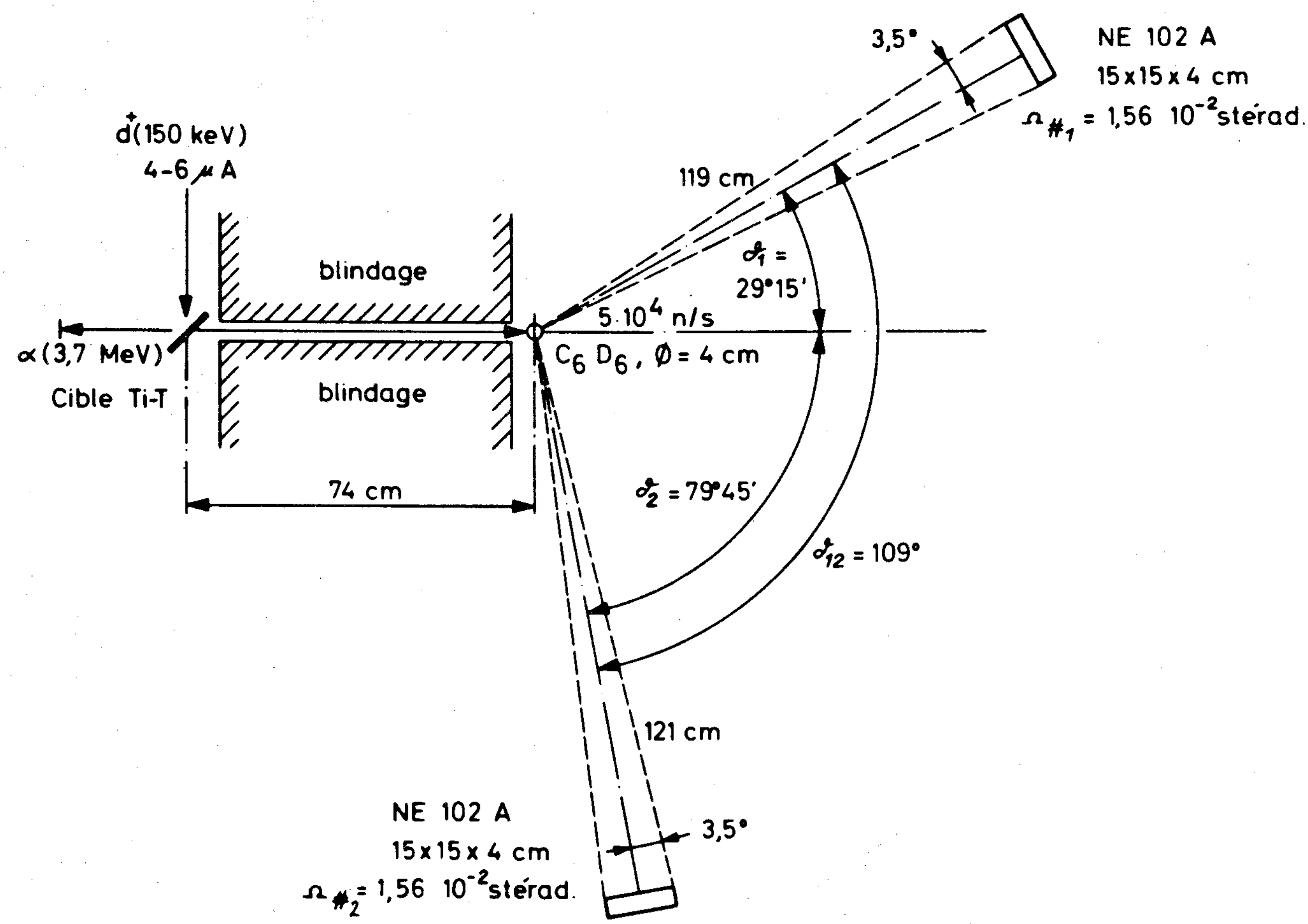

Fig. 9:

Experimental arrangement for the complete experiment on D(n, 2n)H.

(time of flight) and E_p (scintillation) gives a double redundancy. This is essential for the elimination of false coïncidences distributed in the E_1E_2 plane outside of the kinematical curve.

A careful selection of events gives the distribution of Fig. 10 for the projection on the E_1 axis. Position and form of the peak, corresponding to the n-p pole, are given correctly by a Watson-Migdal [1] type of theory, after normalisation to the peak area on the energy interval corresponding to $E_{13} \leq 300$ keV and using the given values for a^s_{np} and r^s_o.

Several systematical tests of variation of the experimental parameters within their limits of imprecision have shown that the value of a_{np} stabilizes around -20 fm.

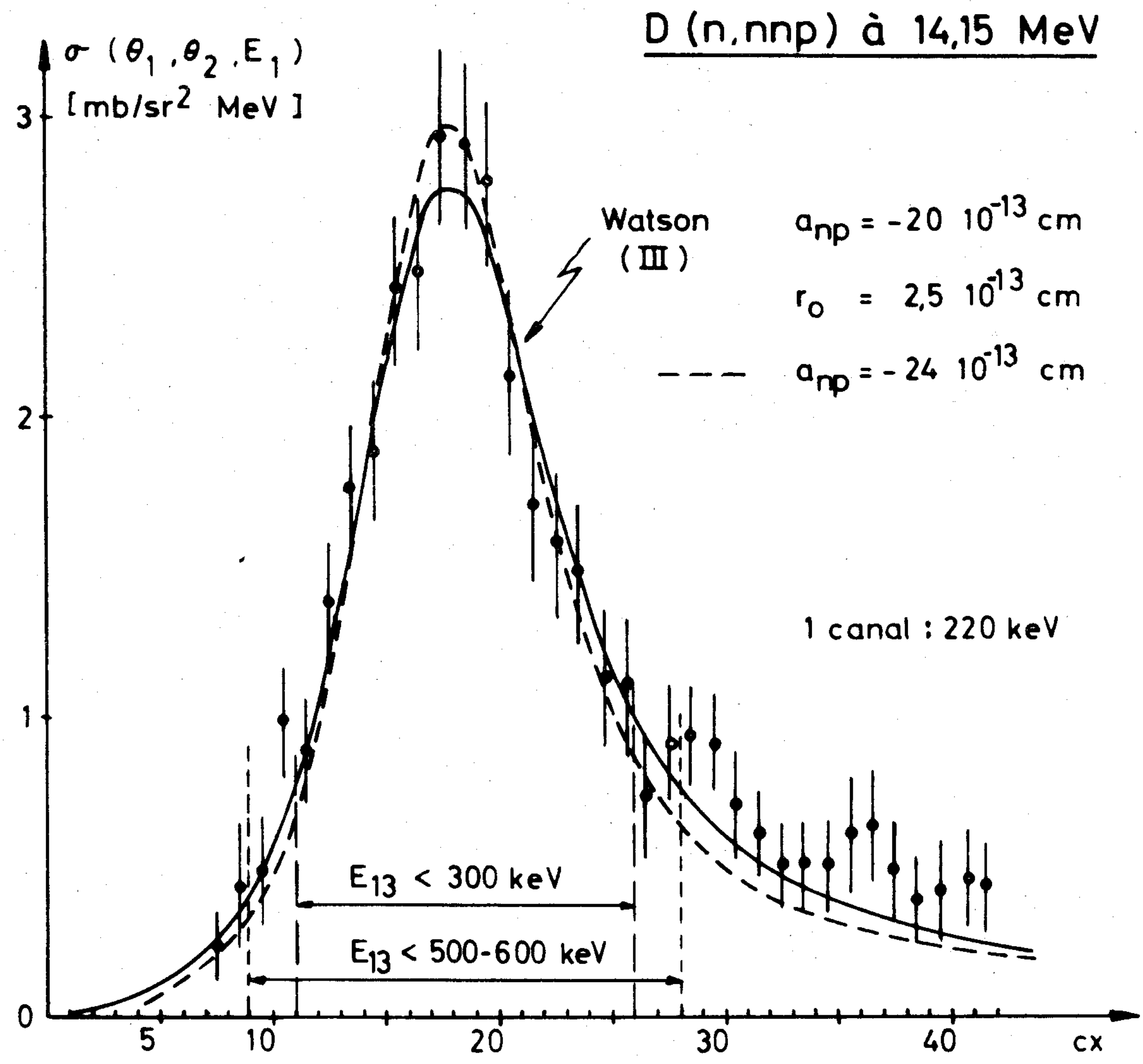

Fig. 10:

Distribution of events projected on the E_{n1}-axis.

A more complete theoretical interpretation has been tried with the Feynman graphs method (Komarov-Popova [2]) at the pole diagram approximation. The five contributions to the matrix element (triplet and singlet np, singlet nn and permutation of particles in the final state) are given in Fig. 11.

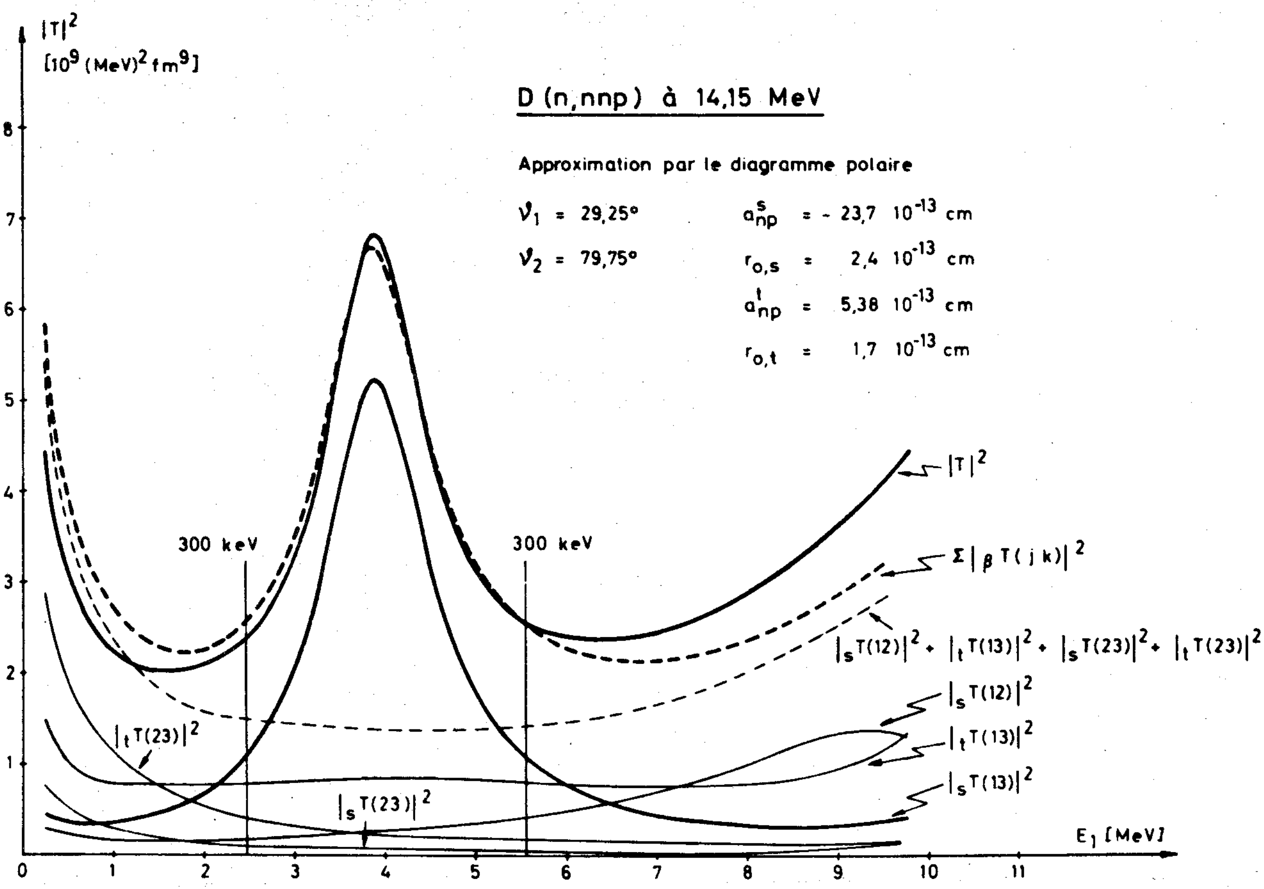

Fig. 11:

Contribution of five matrix elements analysed by pole diagram approximation.

It can be seen that the (1, 3) singlet is dominant. The interference effects ($|\Sigma\ T_i|^2 - \Sigma |T_i|^2$) are small and the other contributions are essentially constant in the domain of interest for this study.

This suggests a correction given by the subtraction of a constant contribution for the matrix element square which can be estimated as at most 10%. Adjusting then the Watson curve with a χ^2 test gives for a_{np} a value shifting from -20 to -23 fm.

Effective calibration of the incident neutron flux and of the absolute efficiency of the neutron detectors using comparison with D-D neutrons from the 3 MeV van de Graaff machine, gives the differential cross section in the vicinity of the n-p pole. One obtains $d^3\sigma/d\Omega_1 d\Omega_2 dE_1$ = 3.1 ± 0.3 mb $sr^{-2}MeV^{-1}$ in good agreement with the result of Perrin et al. [3] . (The calculated value is between 5 and 6 times higher.)

This analysis of our results leads us to the following conclusions:

- A measurement with redundancy is indispensable for a reliable result.
- Location and shape of $\sigma(\theta_1, \theta_2, E_1)$ are explainable in terms of a pole-diagram dominance. The observed discrepancy in form outside the region where $E_{13} < 500$ keV may be reduced by inclusion of triangular graphs, etc.
- The absolute theoretical cross section is still unreliable but this value is necessary for a complete clarification of the mechanism.
- The result $a^s_{np} = -(22 \pm 2)$fm for the 3 body reaction is compatible with $a^s_{np} = -23.7$ fm for the 2 body process (on the energy shell).
- There exists a difference between $|a^s_{np}| > 20$ fm and $|a^s_{nn}| < 20$ fm [3] [4] . This implies a violation of the rule of charge independence of the strong nuclear forces.

This work has been completed with the support of the F.N.S.R.S.

References

[1] K.M. Watson, Phys. Rev. 88, 1163 (1952)

[2] V.V. Komarov and A. Popova, Nucl. Phys. 54, 278 (1964)

[3] C. Perrin et al., Three Body Problem Conference Report, Birmingham (1970), pg 26

[4] R.P. Haddock et al., Phys. Rev. Letters 14, 318 (1965)
B. Zeitnitz et al., Phys. Letters 28B, 420 (1969)

3. Polarization Measurements in the D(n, n) Scattering at 2.5 MeV* (Preliminary Analysis)

R. Viennet, J. Piffaretti and J. Weber

The neutron polarization has been measured at three angles θ_{Lab}: 45°, 60° and 120°. The data reduction computer code is similar to the one described elsewhere [1]. A rough estimate showed that multiple scattering might be important; therefore a Monte-Carlo computer code has been written which takes into account polarization effects on the first scattering on carbon. This code follows closely the schemes described by Wächter et al. [2] and Joseph [3]. The time-of-flight spectra obtained from the Monte-Carlo are then folded with a Gaussian resolution function (the variance of which is time dependent) in order to fit the experimental spectra. This work is now in progress. The preliminary results are:

θ_{Lab}	Multiple scattering	$P_{measured}$	$P_{corrected}$
45°	5 %	0.009 ± 0.01	0.0095 ± 0.01
60°	10 %	0.036 ± 0.013	0.04 ± 0.013
120°	30 %	0.009 ± 0.013	0.013 ± 0.013

The errors are statistical.

Polarization measurements between 20°_{Lab} and 50°_{Lab} are being prepared. The data from the measurement of P_1 are being analysed and have yet to be corrected for the multiple scattering by using the same Monte-Carlo code. It is expected that the results of Sawers et al. will be essentially confirmed.

A phase shift analysis has been made [4], based on the following data:

1) Total cross section at 1.67 MeV C.M. [5]
2) Nine values of $d\sigma(\theta)/d\Omega$ at 1.63 MeV [6] C.M.
3) The three uncorrected values of P showed in the table above.

*) EANDC(OR)-90 "L", pg. 19 (1969)

The essential assumptions are: channel spin and orbital momentum are conserved; S, P and D phase shifts are taken into account.

Other analysis based on the effective range approximation (ERA) are in progress. They will cover 118 pieces of data which can be found between 0.2 and 2.2 MeV (C.M.).

The computer code MINDEF [7] has been used to obtain the best fits.

The results are presented in the figures 12 and 13.

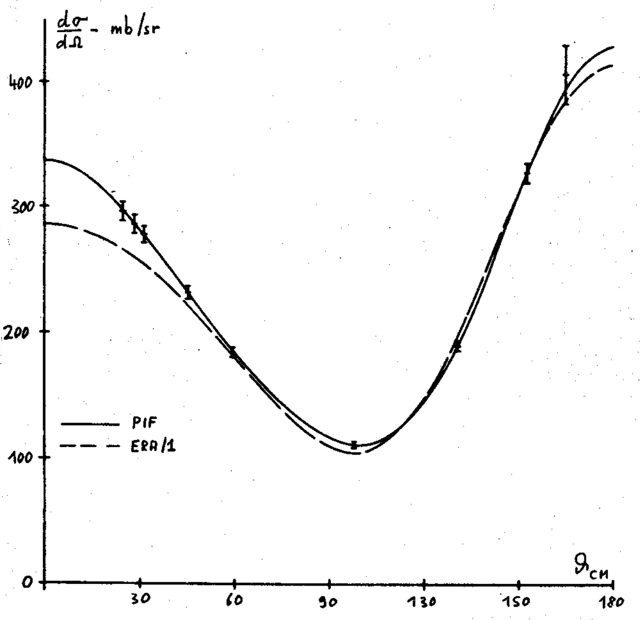

Fig. 12:

Differential d-n-scattering cross section at 2.5 MeV, fits of data.

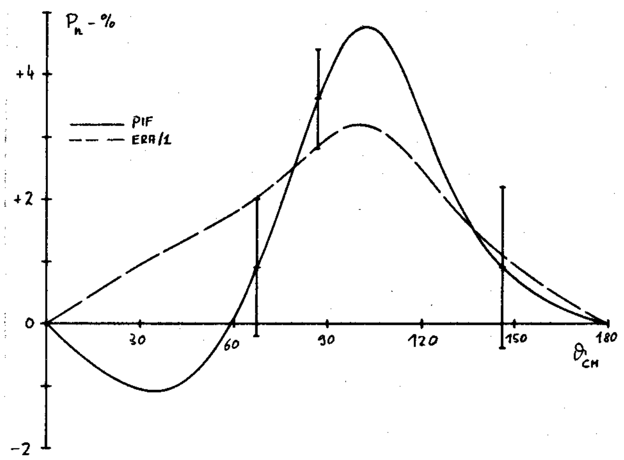

Fig. 13:

Neutron polarization of 2.5 MeV neutrons scattered by deuterium.

References

[1] M. Wächter, M.I.T. Thesis (1962)

[2] M. Wächter et al., N.I.M. 24, 316 (1963)

[3] C. Joseph, Lausanne Thesis (1966)

[4] R. Viennet, J. Piffaretti and J. Weber, Helv. Phys. Acta (to be published)

[5] J.D. Seagrave, R.L. Henkel, Phys. Rev. 98, 666 (1955)

[6] J.D. Seagrave, L. Cranberg, Phys. Rev. 105, 1816 (1957)

[7] J. Beiner, 1969 (unpublished)

4. Treiman-Yang Criterion in the H(d, 2p)n Reaction at E_d = 20 MeV

R. Corfu, J.P. Egger, C. Lunke, C. Nussbaum, J. Rossel, E. Schwarz
(Institut de Physique, Université de Neuchâtel)

and

J.L. Durand and C. Perrin
(Institut des Sciences Nucléaires, Grenoble)

The Feynman graph method applied to light nuclei reactions (Shapiro [1]) advocates the decomposition of the reaction amplitude in a sum of particular diagrams. The possible dominance of the pole graph in a favorable kinematical situation can be elegantly tested with the Treiman-Yang rotation [2]. The pole diagram for the deuteron fracture by a proton is described in Fig. 14. The matrix element depends only on the transferred momentum $\vec{q}$ and on the relative energy f^2 of the proton p_2 and neutron.

If counter p_1 is maintained fixed and counter p_2 moved in such a way as keeping f^2 constant, the matrix element should remain constant, if however the spin of the transferred particle is $\leq \frac{1}{2}$. The corresponding displacement is represented in Fig. 15.

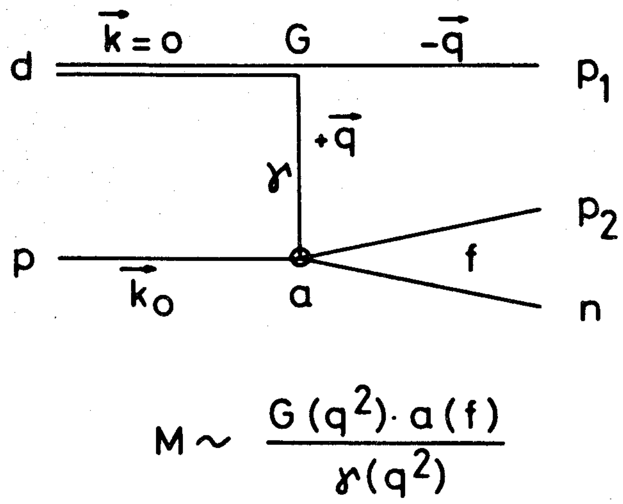

Fig. 14:
Pole diagram for p+d → p+p+n.

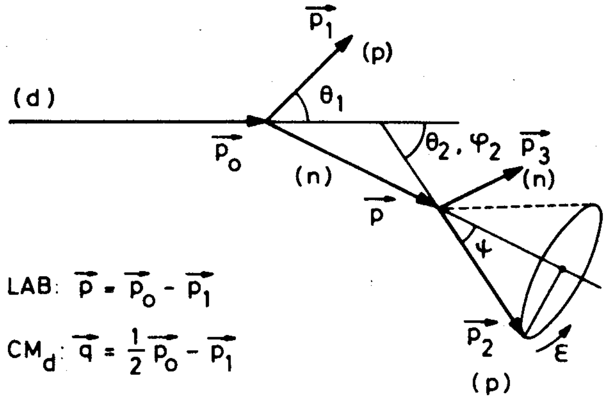

Fig. 15:
p+d → p+p+n, diagram of momenta.

Proton momentum $\vec{p}_1$ fixed means that the transferred neutron carries a well defined momentum $\vec{p} = \vec{p}_o - \vec{p}_1$ in the lab. system. Counter 2 is successively placed at different rotation angles ε around $\vec{p}$ on a cone with fixed angular aperture ψ.

The acceptable configurations (θ_2, ϕ_2) must respect certain theoretical and experimental conditions (small transferred momentum; energy of detected particles sufficiently high, favorable angles for the detection etc.). The 3 chosen configurations define the 3 kinematical curves given in Fig. 16.

For the experiment we used a CH_2 target placed on the 20 MeV deuteron beam of the isochronous cyclotron of Grenoble. The protons are detected by two ΔE-E telescopes (Si surface detectors) placed within a spherical reaction chamber of 1.2 m in diameter which allows motions out of the reaction plane. The energy of the coincident events is analysed and recorded in the form of 5 simultaneous parameters on the magnetic type of a PDP 9 data acquisition system.

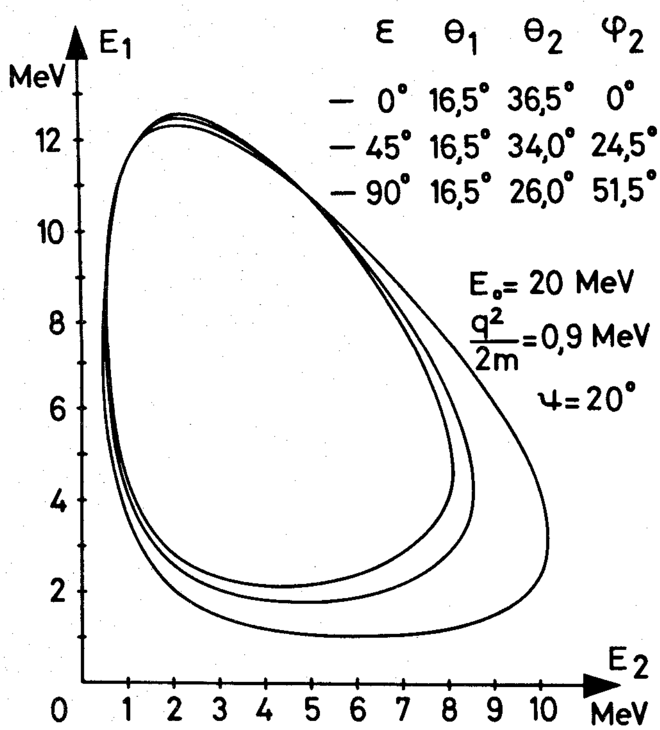

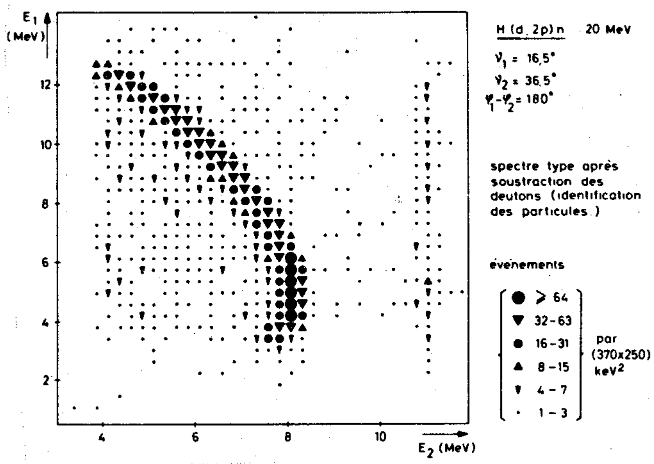

Fig. 16:

Kinematical curves for the reaction $p+d \rightarrow p+p+n$.

Fig. 17:

Measured spectrum in the E_1-E_2-plane.

Fig. 17 shows a spectrum obtained after elimination of unwanted events by particle identification. For each angle ε, the points situated along the kinematical curve are projected on the E_1 axis (spectator proton energy).

The differential scattering cross-sections in the E_1 region which correspond to a small momentum transfer q must be invariant for a rotation ε, if the T-Y criterion is fulfilled.

Up to now we have analysed results obtained for two angles $\varepsilon = 0^\circ$ and $\varepsilon = 90^\circ$ (Fig. 18). In our case 10 MeV $\leq E_1 \leq 11$ MeV corresponds to a small momentum q ($\frac{q^2}{2m} = 0.9$ MeV is small compared with the deuteron binding energy). It may be seen that the cross-sections are very near each other in this region. The smooth curves are the predictions given by the pole graph (Komarov and Popova [3]); the theoretical values are too high and have been here divided by an arbitrary factor of 4.

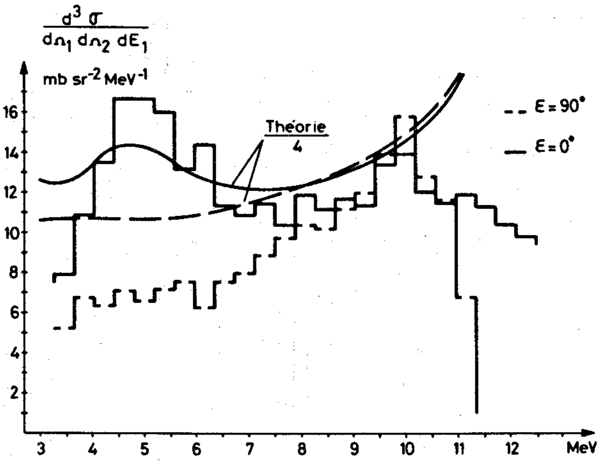

Fig. 18:

Preliminary evaluation of the differential scattering cross section.

These preliminary results seem to indicate fulfilment of the Treiman-Yang criterion.

More precise conclusions will be hopefully drawn from further measurements which are now in progress.

References

[1] I. S. Shapiro
Some Problems of the Theory of Nuclear Reactions at High Energy.
Proc. Int. School of Physics "Enrico Fermi", Course 38 (1967), Academic Press, N. Y.

[2] I. S. Shapiro, V. M. Kolybasov, G. R. Augst,
Nucl. Phys. 61, 353 (1965)

[3] V. V. Komarov, Anna M. Popova,
Nucl. Phys. 54, 278 (1964)

II. Physikalisches Institut der Universität Basel

(Dir.: Prof. Dr. Paul Huber)

1. $^{14}N(n, \alpha)^{11}B$ and $^{12}C(n, \alpha)^{9}Be$ Reactions at Neutron Energies Between 14.8 and 18.8 MeV

W. Salathe, E. Baumgartner and P. Huber

Thin ^{14}N and ^{12}C targets have been bombarded with neutrons at 30 neutron energies between 14.8 and 18.8 MeV. The energy-spread of the neutrons has been 60 keV. The differential cross sections of $^{14}N(n, \alpha_o)^{11}B$, $^{14}N(n, \alpha_1)^{11}B^*$ and $^{12}C(n, \alpha_o)^{9}Be$ were obtained at 9 various angles between 0 and 156 degrees (CM) (Fig. 19, 20, 21).

The measurements were undertaken to decide if the reactions proceed via direct processes. An analysis using direct reaction theory is in progress.

2. Polarization of Neutrons from the $D(d,n)^{3}He$ Reaction with Vector Polarized Deuterons

A. Janett, P. Huber, U. von Möllendorff and H. R. Striebel

In the $D(d,n)^{3}He$ reaction the influence of the deuteron vector polarization on the transverse component of the neutron polarization has been investigated at the emission angles of 110^o and 90^o. For a mean reaction energy of 460 keV we have measured with polarized and unpolarized deuterons alternatively. The neutron polarization has been determined by the azimuthal asymmetry of the elastic scattering from the carbon contained in a first plastic scintillator. The scattered neutrons have been detected by two other scintillation counters in coïncidence with the ^{12}C-recoils.

The results obtained so far show that the contribution to the n-polarization proceeding from transverse vector polarization of the deuterons changes sign at an angle near 110^o, whereas the contribution from longitudinal

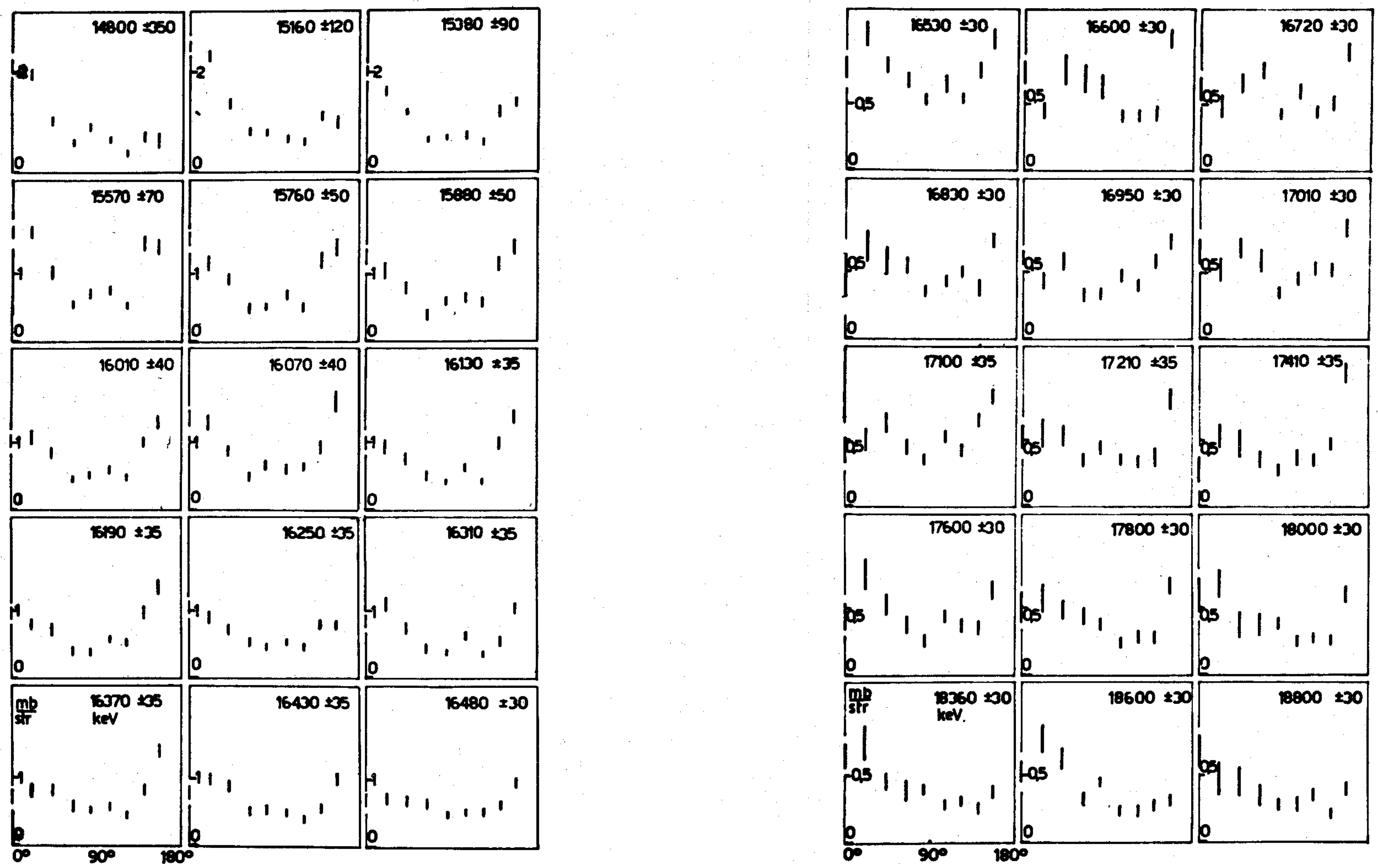

Fig. 19:

Differential cross sections of $^{14}N(n, \alpha_o)$ in the CM-system at the angles 0^o, 22^o, 44^o, 65^o, 85^o, 104^o, 122^o, 140^o, 156^o. The neutron energy and the neutron-energy-spread are in keV, the cross sections in mb/sterad.

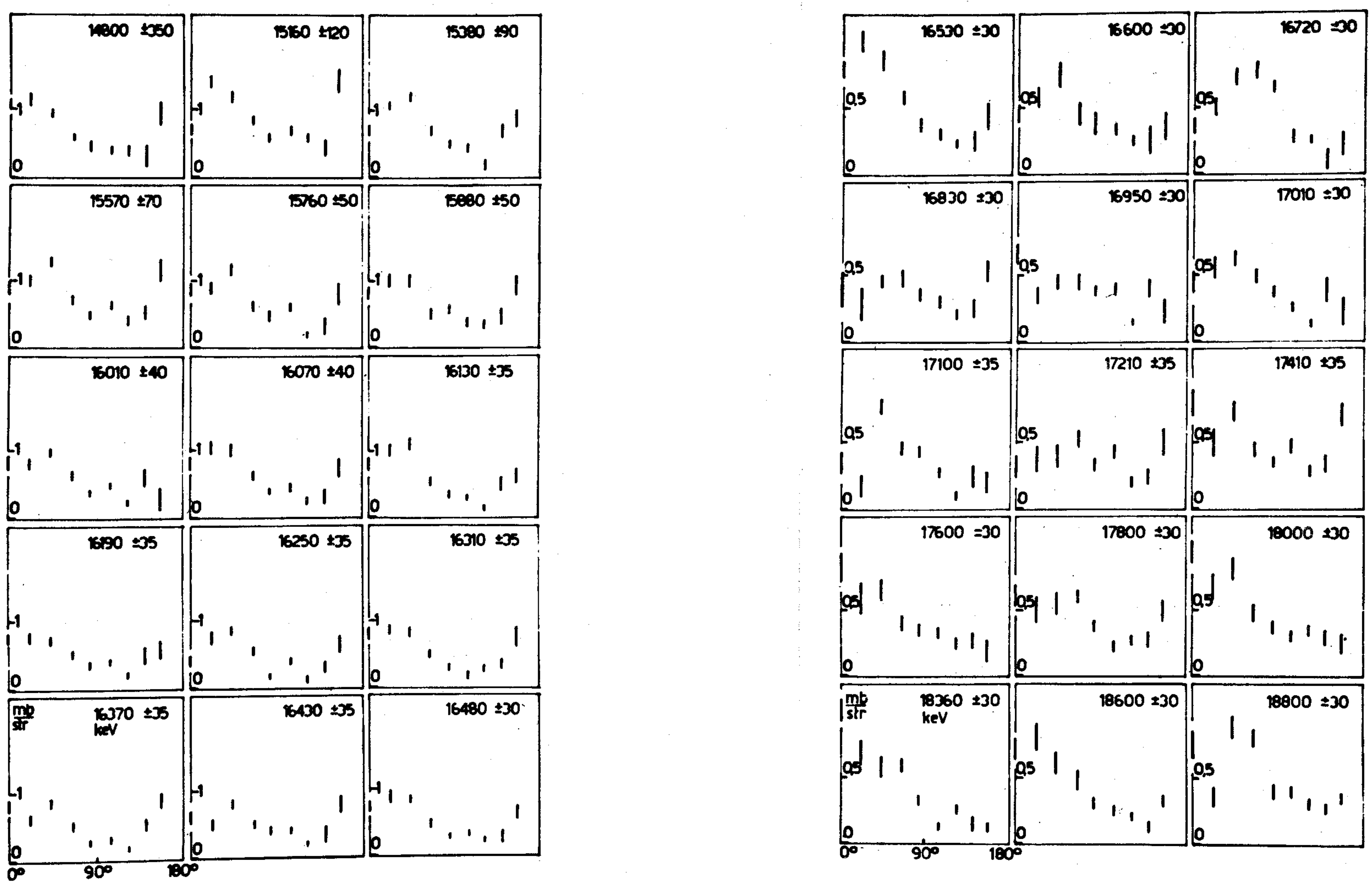

Fig. 20:
Differential cross sections of $^{14}N(n,\alpha_1)$ in the CM-system at the angles $0^o, 22^o, 44^o, 66^o, 86^o, 105^o, 123^o, 140^o, 157^o$.

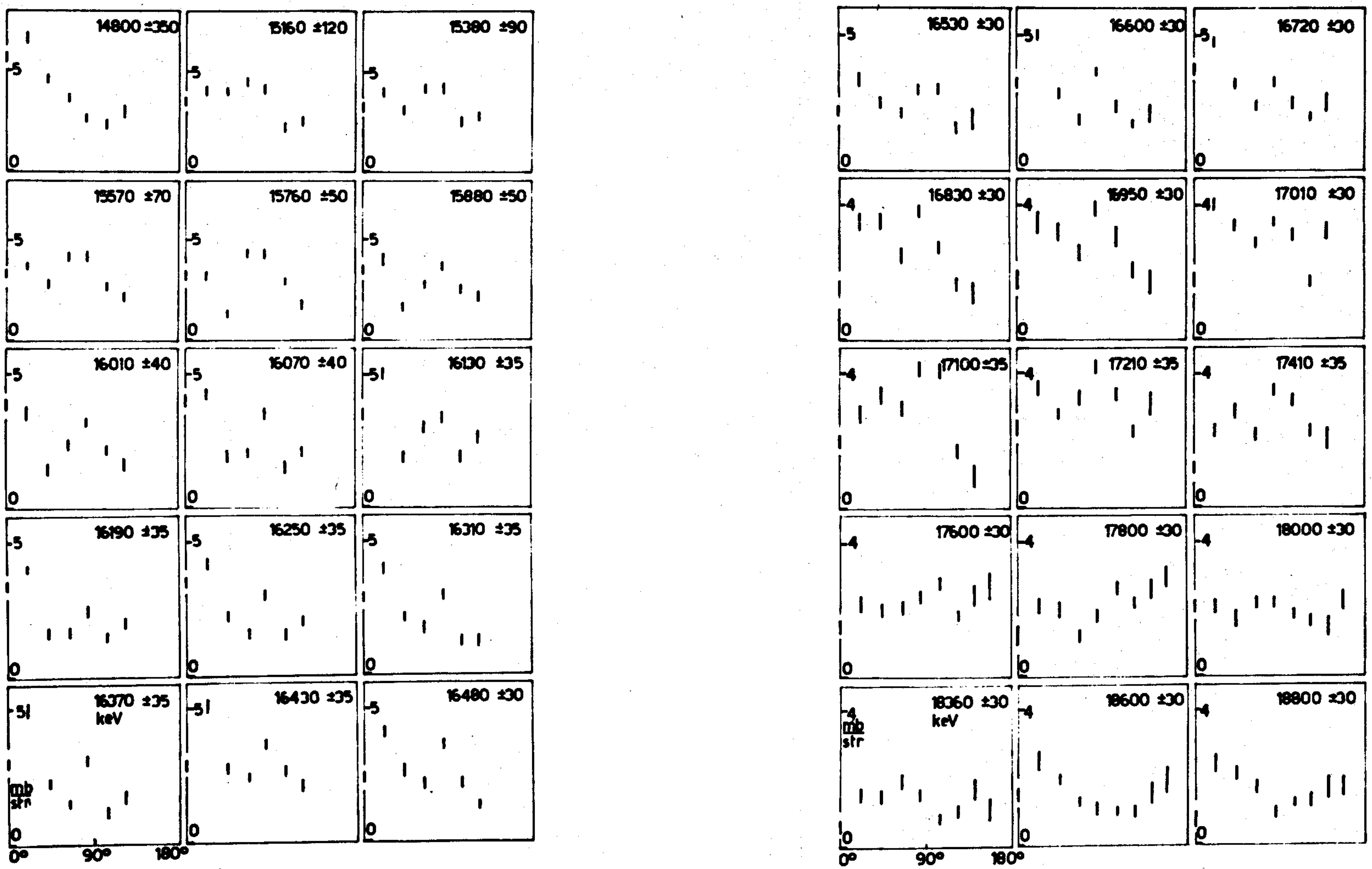

Fig. 21:
Differential cross sections of $^{12}C(n,\alpha_o)$ in the CM-system at the angles 0°, 24°, 47°, 69°, 90°, 109°, 127°.

deuteron polarization differs from zero at 110°. The polarization values are generally quite small ($P_n \leqslant 15\%$ for $P_d = 1$) what for the present can only be explained by the great number of reaction matrix elements.

As a check of the experimental method, the neutron polarization from our data with the unpolarized deuteron beam was evaluated using the analysing power of ^{12}C according to Wills et al. [1] . The result of $(10 \pm 2)\%$ at 110° is in accordance with the data of several authors [2] . The zero effect found at 90° indicates that the instrumental asymmetry has been eliminated correctly.

References

[1] J.E. Wills et al., Phys. Rev. 109, 891 (1958)

[2] H.J. Boersma et al., Nucl. Phys. 46, 660 (1963);
J.P.F. Mulder, Phys. Lett. 23, 589 (1966);
A.F. Behof et al., Nucl. Phys. A 108, 250 (1968).

3. The $^{7}Li(d,n)^{8}Be$ Reaction with Polarized Deuterons

U. von Möllendorff, P. Huber, A. Janett, S.M. Rizvi and H.R. Striebel

The neutron spectrum of the $^{7}Li(d,n)^{8}Be$ reaction at deuteron energies below 1 MeV shows two neutron groups at $E_n = 15$ and 12 MeV, corresponding to the ground and first excited states of the ^{8}Be nucleus respectively, and possibly also a weak background continuum due to the process $^{7}Li + d \rightarrow \alpha + \alpha + n$. Using plastic scintillation counters the two groups can be separated by pulse height discrimination. We have measured the angular distributions of the analysing power of the ground state reaction for the vector and tensor polarizations of the 800-keV deuteron beam, using a target of saturation thickness.

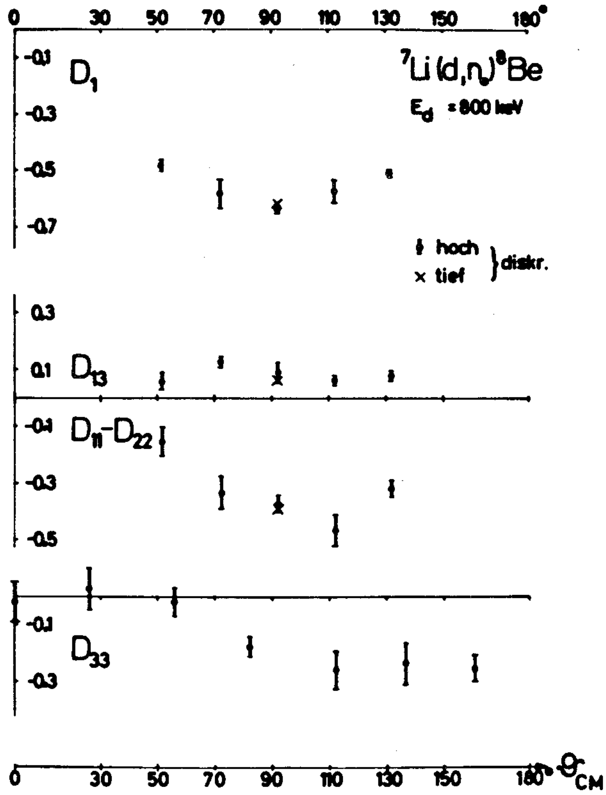

Fig. 22:

Measured vector and tensor analysing power of the $^7Li(d,n_0)^8Be$ reaction.

The data obtained so far are shown in Fig. 22. At reaction angles between 50^o and 130^o the vector analysing power is negative and almost sinusoidal with absolute values up to 2/3. The components of the tensor analysing power at these angles are smaller and the angular dependence is more intricate.

4. The $^{11}B(d,n)^{12}C$ Reaction with Polarized Deuterons

S. M. Rizvi, P. Huber, U. von Möllendorff, F. Seiler and H. R. Striebel

The components of the polarization efficiency of the $^{11}B(d,n)^{12}C$ reaction have been measured at 900 keV mean deuteron energy using a source of polarized deuterons. The two neutron groups corresponding to the ground and first excited states of the ^{12}C-nucleus are easily separated because of the large energy difference of 4.4 MeV and the difference of cross sections. The high energy β^--particles (E_{max} = 13.37 MeV) from the reaction $^{11}B(d,p)^{12}B \rightarrow {}^{12}C + \beta^-$ have been eliminated by lead absorbers in front of the plastic scintillators. The measured components of the polarization efficiency and their fits by Legendre polynomial expansions are shown in Fig. 23.

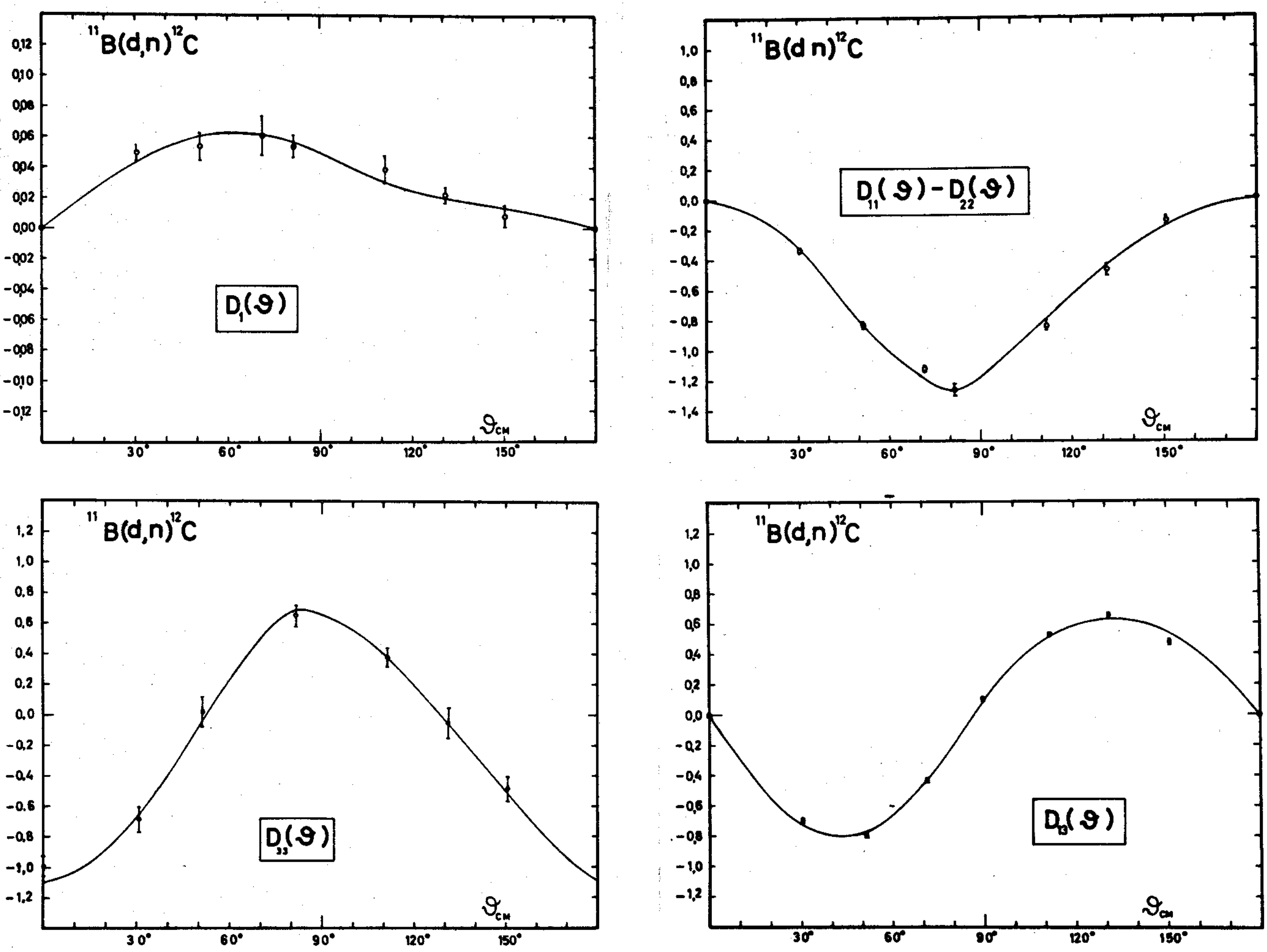

Fig. 23:

Components of the polarization efficiency for the reaction $^{11}B(d,n_o)^{12}C$ at E_d = 900 keV, fitted by Legendre polynomials.

The results show besides the predominating s-wave that there are some p- or d-wave contributions as well. The large s-wave contribution hints at a $3/2^-$ -resonance. The energy levels of ^{13}C above 16 MeV are not well known. The 0^o excitation curves for the neutrons leaving the ^{12}C-nucleus in the ground state show a broad maximum at $E_d = 1.45$ MeV [1], [2]. According to our measurements the resonance would correspond to a $3/2^-$ level in ^{13}C at 20.13 MeV.

References

1 G.U. Din, M.A. Nagarajan and R. Pollard, Nucl. Phys. A 93, 190 (1967)

2 P.R. Almond and J.R. Risser, Nucl. Phys. 72, 436 (1965)

5. Angular Distributions of the $^3He(d,p)^4He$-Reaction Between 2.8 and 10 MeV Using a Polarized ^3He-Target

Ch. Leemann, P. Huber, H. Meiner, U. Rohrer, J.X. Saladin and F. Seiler
(Physikalisches Institut der Universität Basel)

and

W. Grüebler, V. König und P. Marmier
(Laboratorium für Kernphysik der ETH, Zürich)

The left-right asymmetry $A(\vartheta)$ produced by an optically pumped ^3He-target (polarization of approx. 20%, pressure 4 torr) and an unpolarized deuteron beam of about 300 nA was measured at 16 angles and 6 deuteron energies between 2.8 and 10 MeV. In this region the maxima of $A(\vartheta)$ rise from 20 to 70% of the maximum value. As in the mirror reaction $T(d,n)^4He$ structural changes were found at 4 and 6 MeV considerable odd-parity contributions are found. A detailed analysis is in progress.

III. Institut de Physique Nucléaire, Université de Lausanne

(Dir.: Prof. Dr. Ch. Haenny)

1. (n, Charged Particles) Reactions at 14.0 MeV

J.F. Loude, J.P. Perroud, Ch. Sellem

The differential cross section of the $^{12}C(n, \alpha_0)^9Be^f$-reaction has been measured at several angles with the spectrometer described in [1]. Measurements carried out in the forward hemisphere give values between 3 and 6 mb/sr.

One preliminary measurement of the reaction on ^9Be at 0^o has been completed. A triparametric analysis of the events (rest energy, time of flight, energy loss) allows unambiguous identification of the emitted charged particles: tritons, alpha particles, ^6He.

The measured spectra show perfectly resolved peaks which can be attributed to the following particles and reactions:

- 2 alpha rays emitted by $^9Be(n, \alpha)^6He$, leading to the ground and first excited (1.80 MeV) state of ^6He.
- 1 ^6He peak originating from the $^9Be(n, \alpha_0)^6He$-reaction.
- 2 tritium lines from $^9Be(n,t)^7Li$, leaving the final nucleus ^7Li in the ground and first excited (0.478 MeV) state.

The measurement of the complete angular distribution of the reactions $^9Be(n, \alpha)^6He$ and $^9Be(n,t)^7Li$ is in progress.

Reference

[1] J.F. Loude, J.P. Perroud and Ch. Sellem, EANDC(OR)-90"L", pg 15 (1969) and HPA 42, 905 (1970).

2. $^{10}B(n,n)$ and (n,n'), $^{11}B(n,n)$ and (n,n') at 14 MeV

J.C. Alder and B. Vaucher

Measurements on the scattering of 14 MeV neutrons from ^{10}B and ^{11}B have been discussed in last year's report [1]. The results will be published in detail in Helvetica Physica Acta 43, 905 (1970) and Nuclear Physics.

Reference

[1] EANDC(OR)-90 "L", pg. 12 (1969)

IV. Eidgenössisches Institut für Reaktorforschung (EIR), Würenlingen

(Dir.: Dr. A.F. Fritzsche and Dr. W. Zünti)

1. Capture Cross Section Measurements of Vanadium, Manganese, Cesium, Europium, Dysprosium and Lutetium in the Neutron Energy Range from 0.01 eV to 20 eV.

F. Widder

In order to improve the capture data of the elements mentioned above which are contained in the EANDC request list, high precision measurements were run with the neutron chopper installed at the DIORIT reactor of the EIR.

The detector used was of Moxon-Rae type. The converter thickness was optimised and the energy dependent boundary effect in the environment of the scintillator was taken advantage of to achieve good proportionality of the efficiency of the detector with respect to the decay energy (or binding energy of the captured neutron). The calibration measurements have shown good linearity in the γ-energy range from 0.5 MeV to 10 MeV. The critical background measurements with an improved boron-filter method were carefully investigated to ensure high precision. The necessary corrections to the measurements, i.e. multiple scattering, selfshielding and activation of the targets during the measurements, were also taken into account and were calculated with special methods.

The measurements have recently been completed, the evaluations by means of computer programmes are in progress. The results will soon be published in the form of curves as well as tables: $\sigma_c(E_n)$ and $\sigma_s/\sigma_c(E_n)$.

2. The Thermal-Neutron Fission Cross Section of Thorium-227*

H.R. von Gunten, K.F. Flynn and A. Schmid

The thermal-neutron fission cross section of ^{227}Th was measured using both back to back fission counters and radiochemical methods. The sepa-

*) Full paper in J. inorg. nucl. Chem. (in print)

ration of ^{227}Th was performed from a source of ^{227}Ac applying ion-exchange techniques followed by molecular plating of the samples. Very uniform thin targets were obtained. The number of ^{227}Th atoms in the samples was measured with a calibrated GeLi-detector using the 236 keV γ-peak which is 10.35% abundant [1] . The fission counting was performed with a parallel plate type fission counter at a beam hole of the SAPHIR swimming pool reactor in a thermal neutron flux of $5 \times 10^{8} cm^{-2} sec^{-1}$. The fast component in the beam was approximately 1/10 of this value. A Cd-metal-sheet of 1 mm thickness reduced the count rate in the ^{227}Th-sample by a factor of 12 compared to a factor of 32 for the ^{235}U-sample. The fission count rate of the ^{227}Th decreased with a half-life of 18.7 days, which proves that the measured fission events are due to ^{227}Th.

In the radiochemical experiments we compared the count rates of the isolated fission products ^{95}Zr, ^{111}Ag, ^{132}Te, ^{141}Ce and ^{143}Ce from a ^{227}Th sample to those of the same fission products from a ^{235}U sample which was irradiated together with the ^{227}Th. Known fission yields for ^{227}Th from [2] and for ^{235}U from [3] were used in these calculations.

The results of 7 counter experiments and a mean value of 5 radiochemical determinations using the fission products mentioned above are shown in Table 1. A weighted mean for the value of

$$\sigma_{f}(^{227}Th) = 200 \pm 20 \text{ barns}$$

was obtained. This value is in agreement with our preliminary result $\sigma_{f}(^{227}Th) = 250 {}^{+200}_{-100}$ barns [4] , but it disagrees considerably with the published value of 1500 ± 1000 barns [5] .

References

[1] W.F. Davidson and R.D. Connor, Nucl. Phys. A 116, 342 (1968)

[2] K.F. Flynn and H.R. von Gunten, Proc. 2nd Conf. on Physics and Chemistry of Fission, IAEA, Vienna (1969) 731

[3] M.E. Meek and B.F. Rider, APED-5398-A (1968)

[4] K.F. Flynn and H.R. von Gunten, EANDC-(OR)-75 "L", pg 27 (1968)

[5] D.J. Hughes and J.A. Harvey, BNL 325 (1955)

Table 1: Results of the Experiments for the Determination of the Thermal-Neutron Fission Cross Section of Thorium-227

Type and No. of Experiment	Atoms of ^{227}Th used $\times 10^{13}$	Duration of Experiment days	Number of Points Measured	Background of Counter counts/sec	Net Fission Count Rate of ^{227}Th at Zero-Time counts/sec	Fission Count Rate of ^{235}U $(4.31 \pm 0.08) \times 10^{15}$ Atoms counts/sec	σ_f Fission Cross Section of ^{227}Th barns
Counter 1	4.83 ± 0.5	18	51	0.05 ± 0.01 [a]	0.04 ± 0.01	12 ± 1	172 ± 44
Counter 2	0.265 ± 0.03	15	52	0.03 ± 0.006 [a]	0.03 ± 0.009	135 ± 2	209 ± 67
Counter 3	1.00 ± 0.10	7	30	0.013 ± 0.003	0.06 ± 0.01	88 ± 1	170 ± 34
Counter 4	0.36 ± 0.04	4	18	0.02 ± 0.004	0.03 ± 0.008	120 ± 2	171 ± 48
Counter 5	0.095 ± 0.01	15	66	0.05 ± 0.01	0.010 ± 0.003	146 ± 3	181 ± 55
Counter 6 [b]	1.31 ± 0.13	55	245	0.01 ± 0.002	0.14 ± 0.004	133 ± 2	228 ± 24
Counter 7 [b]	1.26 ± 0.13	11	43	0.01 ± 0.002	0.18 ± 0.01	168 ± 2	212 ± 25
Radio-chemical [c]	0.63 ± 0.07	3 [d]	5	---	---	---	188 ± 47

σ_f Weighted Mean : 200 ± 20 barns

a) Difficulties with α-pileup
b) 2nd source of ^{227}Ac used in these experiments
c) Mean values from 5 independent determinations
d) Time of irradiation

3. Distribution of Mass and Charge in the Thermal-Neutron-Induced Fission of ^{249}Cf *

K.F. Flynn and H.R. von Gunten

The distribution of mass and charge in the thermal-neutron-induced fission of ^{249}Cf has been investigated by radiochemical determination of the fission yields of 25 mass chains and one shielded nuclide (independent yield). The mass distribution is asymmetric, as in all known cases of low-energy fission. The heavy-mass group is centered at mass number 139, the light-mass group at 106. The peak-to-valley ratio is higher than 30. The full width at half maximum (FWHM) is 16 mass units; at one tenth maximum it is estimated to be 28 mass units. The mass distribution can be reflected at mass 122; this indicates a value of 6 ± 1.5 for $\bar{\nu}$, the average number of neutrons emitted per fission. The division of nuclear charge, as indicated by the independent yield of ^{136}Cs is consistent with the equal charge displacement hypothesis characteristic of low energy fission.

The results of the fission yield determinations are shown in Table 2. The independent fission yield and the corresponding value for Z_p is given in Table 3.

*) Full paper published in Helv. Chim. Acta 52, 2216 (1969).

Table 2: Fission yields in the thermal-neutron induced fission of ^{249}Cf

Fission product	Method of counting	Number of determinations	Fission yield %
^{92}Sr	β, γ	1	1.17 ± 0.29
^{95}Zr	β, γ	3	1.72 ± 0.26
^{97}Zr	β, γ	3	2.35 ± 0.46
^{99}Mo	β, γ	4	3.42 ± 0.24
^{103}Ru	β, γ	3	5.27 ± 0.62
^{105}Ru	β, γ	2	5.49 ± 0.66
^{106}Ru	β	3	5.09 ± 1.01
^{109}Pd	β	1	4.92 ± 1.23
^{111}Ag	β, γ	8	5.16 ± 0.56
^{112}Pd	β	3	3.48 ± 0.56
^{113}Ag	β, γ	7	2.92 ± 0.32
^{115}Cd	β	4	2.46 ± 0.49
^{121g}Sn	β	3	0.34 ± 0.09
^{125g}Sn	β	6	0.24 ± 0.06
^{127}Sb	β	3	1.23 ± 0.29
^{129m}Te	β, γ	6	2.19 ± 0.33
^{131}J	β, γ	2	3.01 ± 0.45
^{132}Te	β, γ	9	3.95 ± 0.28
^{133}J	β, γ	2	5.09 ± 0.51
^{137}Cs	β	2	6.90 ± 1.03
^{140}Ba	β, γ	4	4.84 ± 1.21
^{141}Ce	β, γ	16	6.34 ± 0.38
^{143}Ce	β, γ	10	4.90 ± 0.28
^{144}Ce	β	10	4.62 ± 0.28
^{147}Nd	γ	2	2.62 ± 0.39

Table 3: Independent fission yield of ^{136}Cs and most probable charge

Independent fission yield for ^{235}U	:	6.0×10^{-3} %
Independent fission yield for ^{249}Cf	:	0.32 ± 0.06 %
Chain yield for ^{249}Cf	:	5.8 %
Fraction of chain yield	:	0.055 ± 0.011
Most probable charge Z_p (empirical)	:	53.5 ± 0.15
Estimated primary mass (A')	:	137.5 ± 0.2 [a)]
$Z_p - A' (Z_F/A_F)$ [b)]	:	-0.40 ± 0.15

a) The number of neutrons emitted by the primary fission fragment is estimated to be 1.5.

b) Z_F/A_F: ratio of charge to mass in the fissioning nucleus = charge density.